Continental Shelf Research 249 (2022) 104852

Contents lists available at ScienceDirect

Continental Shelf Research

journal homepage: www.elsevier.com/locate/csr

# The Natal Bight Coastal Counter-Current: A modeling study

Sonia Heye [a,*], Marjolaine Krug [a,b], Pierrick Penven [c], Michael Hart-Davis [d]

[a] Nansen Tutu Center for Marine Environmental Research, Department of Oceanography, University of Cape, Town, Rondebosh, Cape Town, 7700, Western Cape, South Africa

[b] Department of Forestry, Fisheries and the Environment, Oceans and Coastal Research, 2nd Floor, Forestust Building, Martin Hammerschlag Way, Cape Town, 8002, Western Cape, South Africa

[c] Institut de Recherche pour le Developpement, Laboratoire Oceanographie Physique et Spatiale, IUEM Technopole, Brest Iroise Batiment D, Brest, 29280, Plouzane, France

[d] Deutsches Geodätisches Forschungsinstitut, Technische Universität München, Arcisstraße 21, München, 80333, Bayern, Germany

ARTICLE INFO

*Keywords:*
Natal Bight Coastal Counter-Current
High-resolution ocean model
MPA connectivity
Agulhas Current
Durban Eddy
KwaZulu-Natal Bight

ABSTRACT

Output from a high-resolution ocean model, a wind reanalysis and a particle tracking tool are used to improve our understanding of the shelf circulation in an embayment off South Africa's east coast, known as the KwaZulu-Natal Bight. This region spans across roughly 140 km of coastline and is located between 29°S and 30°S. It is influenced by the strong, south-westward flowing Agulhas Current on its offshore edge, while its shelf is dominated by weak and variable currents. On the KwaZulu-Natal Bight's shelf, realistic high-resolution model simulations indicate the presence of a mean north-eastward flow: the Natal Bight Coastal Counter-Current. The mean surface circulation depicts a Natal Bight Coastal Counter Current stretching along the 50 m isobath from the southern to the northern section of the KwaZulu-Natal Bight while progressively becoming narrower and weaker northwards. The mean vertical structure of this counter current extends throughout the water column and at its origin, it almost connects with the Agulhas Undercurrent. In this region, the Natal Bight Coastal Counter-Current is about 20 km wide and has an average speed of 20 cm/s at its core, which may exceed 100 cm/s during individual events. The passage of southward propagating anticyclonic eddies offshore of the Agulhas Current are associated with a southward flow along the southern KwaZulu-Natal Bight region and the interruption of the otherwise north-eastward shelf currents. While the circulation in the KwaZulu-Natal Bight is primarily driven by perturbations at the Agulhas Current front, there is also some indication of a direct wind-driven influence in coastal waters, inshore of the 50 m isobath and north of 29.5°S. Virtual particle tracking experiments show that the Natal Bight Coastal Counter Current may increase connectivity between Marine Protected Areas within the KwaZulu-Natal Bight, where the current greatly increases the water retention. This may trap nutrients from coastal origins on the shelf, together with any suspended particles such as larvae. Therefore, the Natal Bight Coastal Counter-Current has the potential to increase the suitability of this habitat for larval settlement.

## 1. Introduction

The continental shelf in the northern Agulhas Current region is overall straight and narrow. However, an area known as the KwaZulu-Natal (KZN) Bight acts as an exception. The KZN Bight roughly extends from Richards Bay to Durban and is characterized by a widened shelf with a shallow bay-shaped coast (Fig. 1). The wide shelf forces the deeply extending Agulhas Current offshore, which allows a slow shelf circulation with complex circulation features (Roberts et al., 2016). Together with river inputs, these features increase the nutrient concentration within the KZN Bight (Scharler et al., 2016) and make this region suitable for recruitment and the retention of marine organisms (Beckley and Hewitson, 1994; Hutchings et al., 2002). The KZN Bight supports several phyto- and zooplankton communities (Barlow et al., 2008; Carter and Schleyer, 1992) and it has an abundance of pelagic fish larvae (Beckley and Hewitson, 1994). To assist with protecting this biologically important region, a range of Marine Protected Areas (MPAs) have been established within and around the KZN Bight (Fig. 1a). Conservation benefits are maximised when the underlying circulation connects MPAs (Sale et al., 2005; Andrello et al., 2017). This study aims

* Corresponding author.
*E-mail address:* hyxson001@myuct.ac.za (S. Heye).

https://doi.org/10.1016/j.csr.2022.104852
Received 25 January 2022; Received in revised form 30 August 2022; Accepted 14 September 2022
Available online 26 September 2022

to improve our understanding of the KZN Bight's circulation and its impact on MPA connectivity.

Previous studies provide some insight into the KZN Bight's circulation features. The widened shelf of the KZN Bight that forces the Agulhas Current offshore results in recurring instabilities in the current's trajectory (Elipot and Beal, 2015). These instabilities become downstream propagating meanders, which often have associated eddies. Such frontal instabilities have been described in the Gulf Stream (Gula et al., 2015), in the Brazil Current (Da Silveira et al., 2008), in the Kuroshio Current (Nagano et al., 2019) and in the East Australian Current (EAC) (Archer et al., 2017). In the Agulhas Current, these meanders usually intensify downstream and are referred to as Natal Pulses, but they may also flatten off the Eastern Cape and disappear altogether (Krug and Penven, 2011; Roberts et al., 2010). When meanders and associated eddies form and pass the KZN Bight, they may result in an inshore south-westward and an offshore north-eastward flow on the KZN Bight's shelf (Roberts et al., 2016).

In the absence of large Agulhas Current meanders, a mesoscale cyclonic feature has been observed off Durban. Similar frontal features were also described in the Gulf Stream (Lee et al., 1991). In the KZN Bight, this feature is referred to as the Durban Eddy and is thought to originate from the strong current shear gradient at the inshore edge of the Agulhas Current over the widening continental shelf (Guastella and Roberts, 2016). In its semi-permanent position, the Durban Eddy extends from Durban (29.86°S) to Sezela (30.41°S) and its center is located between the 300 m and 500 m isobaths. In contrast to passing Natal Pulses, the Durban Eddy results in an inshore north-eastward flow that stretches onto the KZN Bight's shelf and has roughly half the velocity of its offshore south-westward flow, which is enforced by the Agulhas Current (Guastella and Roberts, 2016). Even though several studies have focused on the Durban Eddy with the help of *in situ* data (Oliff, 1969; Pearce and AF, 1977; Schumann, 1987; Roberts et al., 2016; Guastella and Roberts, 2016), not much is known about the extent, persistence and vertical structure of its inshore north-eastward flow and how it connects to the remaining KZN Bight. According to Guastella and Roberts (2016), Durban Eddies have no distinct seasonal cycle and vary strongly in strength and rate of downstream propagation.

Durban Eddies persist for a few days and when they reach a certain size, or when the current shear weakens due to a weakening or meandering Agulhas Current, they break off from their semi-permanent position to propagate downstream (Guastella and Roberts, 2016). After a few days, the next Durban Eddy forms. This process may start on the KZN Bight's shelf, where cyclonic features known as swirls may represent premature Durban Eddies (Roberts et al., 2016). These cyclonic shelf features also result in a north-eastward inner shelf flow and may, just like the Durban Eddy, form as a result of the velocity shear between the Agulhas Current and the shelf (Roberts et al., 2016). However, the study by Roberts et al. (2016) relies on temporally and spatially limited data and not much is known about the persistence or drivers of this circulation feature. Studies on the seabed sand particle deposition in the southern KZN Bight suggest that the swirl is also semi-permanent (Green and MacKay, 2016) and it is observed independently of the Durban Eddy (Roberts and Nieuwenhuys, 2016).

The cyclonic features in the southern KZN Bight are associated with upwelling and nutrient replenishment (Roberts et al., 2011), but may also transport nutrient-poor Agulhas Current water onto the shelf along their outer edge (Meyer et al., 2002; Roberts et al., 2016). Cold cored cyclonic eddies are common features at the inshore edge of western boundary currents and contribute to cross-shelf exchange or productivity by driving upwelling. Roughan and Middleton (2002) describe similar cold-cored, cyclonic eddies in the EAC, which favour shelf-edge upwelling due to the local topography when the EAC separates from the coast. The faster the EAC, the stronger the upwelling, which is consistent with observations of the Durban Eddy (Guastella and Roberts, 2016). Similarly, the Brazil Current also has cold-cored cyclonic eddies, which induce shelf-edge upwelling and supply the Southern Brazil Bight's shelf with nutrients (Lima et al., 1996).

In the northern KZN Bight, the shelf is overall wider and shallower than in the southern KZN Bight (Fig. 2) and has a stronger wind influence (Schumann, 1981). Regular along-shore current reversals are described by Gründlingh (1974) and Roberts et al. (2016), who associated them with local wind patterns, while Schumann (1981) describes the prevailing long-shore drift on the KZN coast as south-north and driven by the prevailing south-easterly swell direction. Therefore, some uncertainty exists about the circulation and its drivers in this region. The wind does, however, result in wind-induced upwelling commonly observed along the northern shelf, particularly when north-easterlies exceed 4 m/s and cause coastal Ekman-induced divergence (Roberts and Nieuwenhuys, 2016). On the shelf edge, eddy pumping and Ekman veering are common drivers of upwelling, which can be induced by

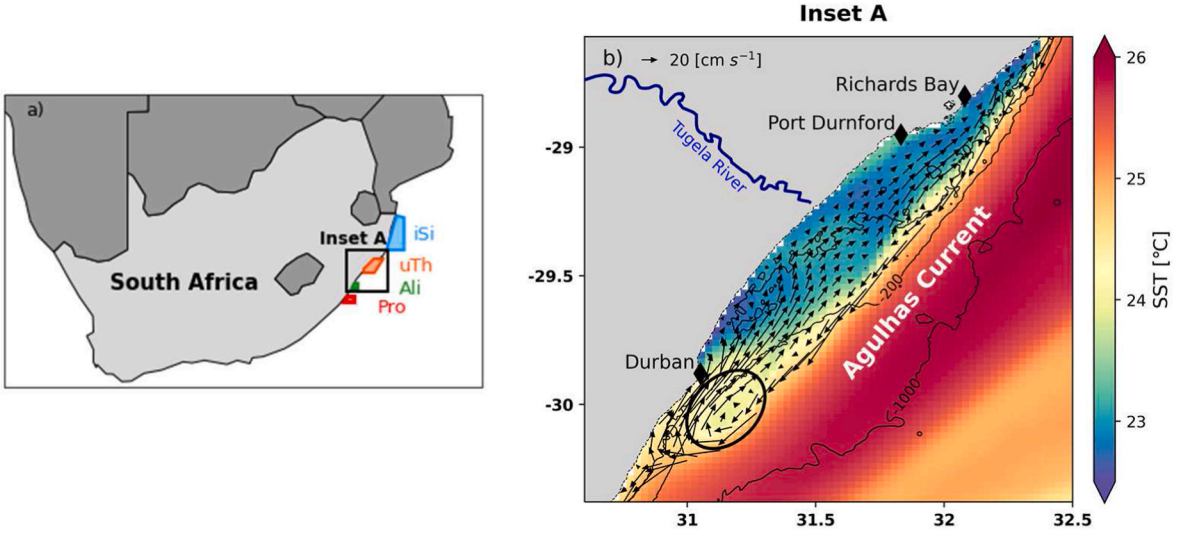


**Fig. 1.** (a) A map of South Africa that indicates the location of the KZN Bight with a black box (Inset A) and the four Marine Protected Areas considered in this study by the colour coded polygons. The blue polygon (labeled 'iSi') is iSimangaliso, the orange polygon ('uThu') is uThukela Banks, the green polygon ('Ali') is Aliwal Shoal and the red polygon ('Pro') is Protea Banks. (b) A zoomed-in map of the KZN Bight. The offshore grey lines are the 50 m, 200 m and 1000 m isobaths. Arrows indicate the surface velocity and the background colour indicates the sea surface temperature (SST) on 21 May 2007, based on CROCO model output. Only velocities weaker than 70 cm/s and inshore of the 1000 m isobath are presented. The black oval in the southern KZN Bight highlights the Durban Eddy location.

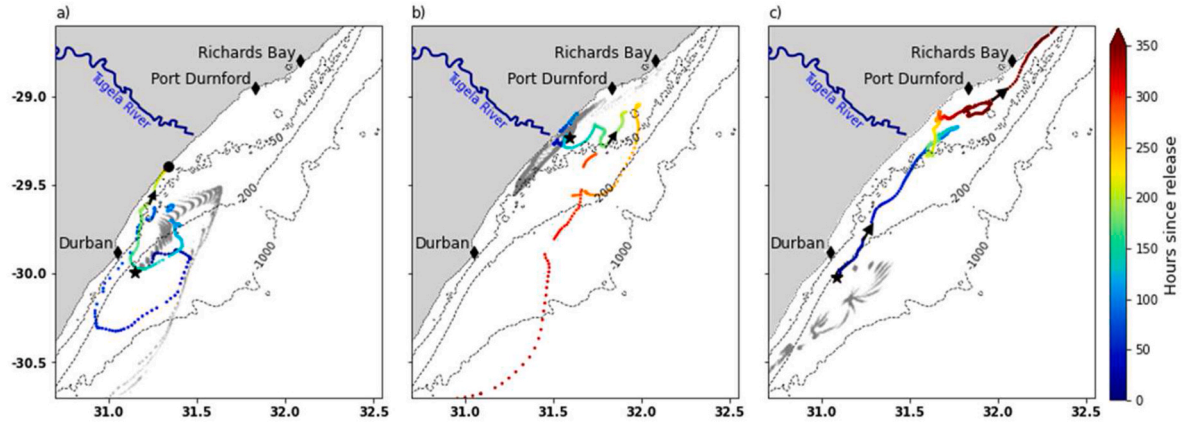


**Fig. 2.** In colour are the trajectories of three NOAA designed drifters that were caught in a north-eastward shelf current in the KZN Bight. Release locations are indicated by black stars and when final locations are within the domain of the map, such as in panel a, they are marked by a black dot. Black arrows show the propagation direction at certain points along the trajectories. The colour of the trajectory is the time since release, measured in hours. Grey dots are the trajectories of 100 virtual particles released in the CROCO model, per panel, at the same location and for the same time period as the drifters.

passing meanders, such as Natal Pulses, or by cyclonic frontal eddies (Roberts and Nieuwenhuys, 2016). According to Roberts and Nieuwenhuys (2016), Ekman veering often works together with wind-induced upwelling and enhances the upwelling events. This is also observed in the Gulf Stream and on the South Atlantic Bight (Pitts and Smith, 1997; Hyun and He, 2010). In the EAC, wind-as well as current-driven upwelling is also observed, where the wind-driven upwelling similarly plays a lesser role (Roughan and Middleton, 2004).

Even though previous studies have focused on the circulation of the KZN Bight, we still lack a coherent understanding. This numerical modelling study presents the opportunity to improve our understanding of the KZN Bight's circulation, with a focus on its vertical structure and drivers, previously gained from scant observations, to help us fill some of the remaining knowledge gaps. A particular focus is on the north-eastward current observed on the KZN Bight's shelf, which originates within the Durban Eddy. It is referred to as the Natal Bight Coastal Counter-Current (NBC3) and an example of such an event is displayed in Fig. 1b. Since the KZN Bight is a biologically important region, the potential biological implications of the NBC3 are also considered. Our ability to understand, model and predict changes in coastal regions, where most human interactions with the ocean occur, relies largely on understanding and documenting the processes which link the deep ocean to the coast. Our study of the KZN Bight and the NBC3 is a contribution to furthering our understanding of the connectivity between the deep ocean and the coastal regions in a region within a western boundary current.

## 2. Methods

### 2.1. Model output

The three-dimensional numerical model used in this study is the Coastal and Regional Ocean COmmunity (CROCO, https://www.croco-ocean.org/). It was built upon the Regional Ocean Modelling System (ROMS_AGRIF) (Debreu et al., 2012) and is a split-explicit free surface model that uses a sigma-coordinate system, meaning that its vertical structure levels follow the topography (Shchepetkin and McWilliams, 2005). Interactions with the topography are explicitly resolved, making it a proper model to address shallow coastal systems such as the KZN Bight (Shchepetkin and McWilliams, 2005). The model numerically solves the Navier-Stokes equations for the ocean dynamics in presence of rotation, following the Boussinesq and hydrostatic approximations (Shchepetkin and McWilliams, 2005).

The Western Indian Ocean Energy Sinks 1/36° resolution CROCO simulation (WOES36) has been created with a special focus on the behaviour of the Agulhas Current and on the representation of the eddy kinetic energy (EKE) in the region (Tedesco et al., 2019, 2022). The model simulation has been compared with altimetry, *in situ* observations from the ACT mooring array (Beal et al., 2015), SAGE glider observations (Krug et al., 2017) and ARGO potential eddy energy (Roullet et al., 2014). Tedesco et al. (2022) show that even though the model EKE is higher than for satellite output along the inshore edge of the Agulhas Current, particularly close to the Agulhas Bank, this difference is no longer observed when the model is smoothed to match the satellite's resolution (Tedesco et al., 2022). They also show that the mean position of the Agulhas Return Current meanders is slightly shifted in the model output. Additionally, Tedesco et al. (2019) show that the mean transport of the Agulhas Current is slightly higher than mooring observations (79.6 vs 77), but the model (WOES36) still performs within the error margin. The model shows an improvement in the representation of the seasonal cycle of Agulhas Current transport compared to previous models (Hutchinson et al., 2018, Fig. 12). WOES36 also has an improved representation of the shear at the inshore edge of the Agulhas Current compared to SAGE glider observations (Tedesco et al., 2019). According to these validations, there is overall a good model-data agreement for the transport and mean vertical and frontal structure of the Agulhas Current, as well as for the eddy variability at the surface and at depth (Tedesco et al., 2019, Figs. 4–6, Tedesco et al., 2022, Fig. 2). Further WOES36 validations are available in the Appendix of a study by Pfaff et al. (2022).

WOES36 has a triple-nested configuration with a two-way nesting approach between the grids (Debreu et al., 2012), ensuring that information is fed from the lower resolution grid into the higher resolution grid and vice versa. The ocean-atmosphere interactions are calculated from daily ERA-Interim atmospheric reanalysis, including the wind stress (Dee et al., 2011), while the bathymetry is derived from the 2014 version of GEneral Bathymetric Chart of the Oceans (GEBCO). The lateral ocean boundary conditions for the large-scale ¼° (25 km) grid resolution 'parent' domain are provided by Mercator global ocean reanalysis GLORYS ¼, which has a daily temporal resolution (Ferry et al., 2012).

Our analysis exploits 10 years of the 1/36° resolution model output from January 2005 to December 2014. The location of the maximum mean north-eastward flow of the model output and on the inshore edge of the Durban Eddy (31.11°E, 29.93°S) is selected and used to identify instances of the Natal Bight Coastal Counter Current (NBC3). NBC3 events are defined by a surface north-eastward flow exceeding 10 cm/s at the above-mentioned location. Using the NBC3 events, a composite representation of the NBC3 surface circulation is created. To gain insight into the temporal variability of the NBC3, a spectral analysis using the

multitaper method is applied to the time-series of the surface flow at the location of maximum mean north-eastward flow. The multitaper method uses adaptive weighting and takes the time-series, its sampling interval and a time bandwidth product set to 6 in this study, to return the power spectrum with its 95% confidence interval. ERA-Interim atmospheric reanalysis which forces the 'parent' grid of the CROCO model is then used to gain a better understanding of the impact of the near-surface wind on the KZN Bight's surface circulation. The impact of the wind is tested by correlating the alongshore and across-shore components of near-surface winds to those of the surface circulation, using the Pearson correlation coefficient.

### 2.2. In situ drifters

Multiple satellite-tracked drifters with the same design as NOAA drifters were released within the KZN Bight and their paths have been analysed by Guastella and Roberts (2016) and Roberts et al. (2016). Three of these drifters that were caught in a north-eastward flow on the shelf are presented in this study in Fig. 2. They were released between April and May of 2010, two of which were deployed off Durban (Fig. 2a and c) and the third off the Tugela River in the KZN Bight (Fig. 2b). The dataset is provided at an hourly temporal resolution (Guastella and Roberts, 2016).

### 2.3. Virtual particle tracking

To complement the output provided by the CROCO model, virtual particles are released within the model using the virtual particle tracking tool Parcels v.2.0 (Probably A Really Computationally Efficient Lagrangian Simulator) (Lange and Sebille, 2017). A detailed description of the set-up of Parcels is provided by Delandmeter and Sebille (2019). The 2D fields of the model proved suitable for implementation in Parcels, which allowed studying the surface layer processes of the CROCO model. This particle tracking tool has been successfully utilised in several studies of the surface dynamics in the Agulhas Current region, such as in search and rescue (Hart-Davis and Backeberg, 2021) and juvenile turtle dispersion (Le Gouvello et al., 2020), indicating its usefulness as a tool to investigate multi-disciplinary issues.

In this study, virtual particles first aimed to represent surface drifters. The model-forced trajectories of 100 virtual particles were compared to the trajectories of the three drifters described in Section 2.2. The virtual particles were released at the same location and for the same time period as the drifters, to allow a direct comparison. However, since the CROCO model is only forced by reanalysis products at the surface (ERA5) and at the lateral boundaries (GLORYS), which are far from the domain of interest, and with the ocean being turbulent, a perfect match between the modelled and real trajectories is not expected.

Next, virtual particles were used to represent passively floating larvae. They were released in four MPAs within and around the KZN Bight, namely iSimangaliso, uThukela Banks, Aliwal Shoal and Protea Banks, as represented in Fig. 1. The virtual particles were tracked over a period of 30 days, with their position outputted every 6 h. The tracking duration was selected to be 30 days since this is the mean pelagic larval duration (PLD) of the larvae of most fish species (Luiz et al., 2013). Virtual particles were released during three northward and three southward flow events within the KZN Bight that were identified as strong and easily identifiable events within the NBC3 time-series, defined in Section 2.1. During the three northward events, virtual particles were released on the 20th of May 2007, on the 25th of June 2009 and on the 17th of April 2013, while during the southward events they were released on the 30th of December 2007, on the 5th of November 2009 and on the 1st of August 2013. The impact of a northward flow on MPA connectivity was investigated using these events. Due to the different spatial extents of the MPAs presented in Fig. 1a, differing amounts of particles were released to keep the particle density similar in the four MPAs. In iSimangaliso, which covers almost 13 300 $km^2$, 20 000 virtual particles were released (roughly 1.5 particles/$km^2$), while in the smaller uThukela Banks MPA that covers roughly 5 670 $km^2$, 10 000 virtual particles were released (roughly 1.7 particles/$km^2$). In each of the smallest MPAs, Aliwal Shoal and Protea Banks that cover 670 $km^2$ and 1 200 $km^2$ respectively, only 2 500 particles were released (roughly 3.7 and 2 particles/$km^2$, respectively). Virtual particles were released evenly throughout the MPA domains that lie within the spatial extent of the model. As the northernmost section of iSimangaliso (north of 27°S) is located outside the model's spatial extent, the particles in this region were not tracked and were excluded from further analysis.

## 3. Results

### 3.1. Horizontal circulation in the KZN Bight

Three satellite-tracked surface drifters released on the KZN Bight's shelf, were caught in a north-eastward shelf flow (Fig. 2). Their velocities rarely exceeded 20 cm/s on the shelf and they had long residence times unless they were caught in the offshore Agulhas Current, which transported them much faster and decreased their residence times. For each drifter, 100 virtual drifters were released at the same time and location and often also moved north-eastwards. The drifter in Fig. 2a was released offshore of Durban. After a cyclonic circulation, it was transported north-eastward onto the shelf, where it remained for about 10 days until it washed up on the beach in the central KZN Bight. The virtual particles in this case were not caught in a cyclonic rotation but also moved north-eastwards into the central KZN Bight until they were advected away by the Agulhas Current instead of beaching. A drifter released in the northern KZN Bight also displayed occasional north-eastward movement on the shelf, where it remained for about 12 days until it was caught in the Agulhas Current and was rapidly advected out of the region with velocities exceeding 100 cm/s on the continental slope (Fig. 2b). The virtual particles released here displayed a similar behaviour, but instead of moving offshore and into the Agulhas Current, they remained along the northern KZN Bight's coast. From these three drifters, the drifter in Fig. 2c, which was also released off Durban, remained suspended on the shelf the longest (over 20 days) until it was retrieved at 28.4°S, near St Lucia and about 200 km north of Durban. This is the only drifter, where virtual particles did not propagate north of Durban but instead underwent a cyclonic rotation and were then advected away by the Agulhas Current.

As already indicated by the model-forced virtual particle trajectories, north-eastward currents over the KZN Bight's shelf are also observed in the surface circulation of the 10-year model output (Fig. 3). A clear distinction in the mean circulation is observed between slow, mostly north-eastward shelf currents (roughly inshore of the 200 m isobath) and fast south-westward currents on the continental slope (between the 200 m and 1000 m isobaths). The persistence of the north-eastward flow is emphasised in the composite of the north-eastward surface circulation in Fig. 3b and d.

Both, the mean and the composite plots, display the Durban Eddy as a prominent circulation feature (Fig. 3). Its associated inshore north-eastward flow stretches throughout the KZN Bight's mid-shelf into the northern KZN Bight, which matches the trajectory of surface drifters in Fig. 2. The signature of the north-eastward shelf flow is also observed at 50 m depth, where it is associated with lower water temperatures at its origin. This cool water is transported north into the KZN Bight region and is particularly evident in the composite plot (Fig. 3d). The mean shelf surface flow overall rarely exceeds 10 cm/s, but is stronger in the composite north-eastward circulation, where it exceeds 30 cm/s in the Durban Eddy region. At the location used for the composite calculations and marked by the cross in Fig. 3b, velocities reached 156 cm/s during the strongest north-eastward event. A maximum inshore north-eastward speed of 93 cm/s is observed in a similar location during the period sampled by Guastella and Roberts (2016).

The KZN shelf region can be divided into an inner shelf (inshore of

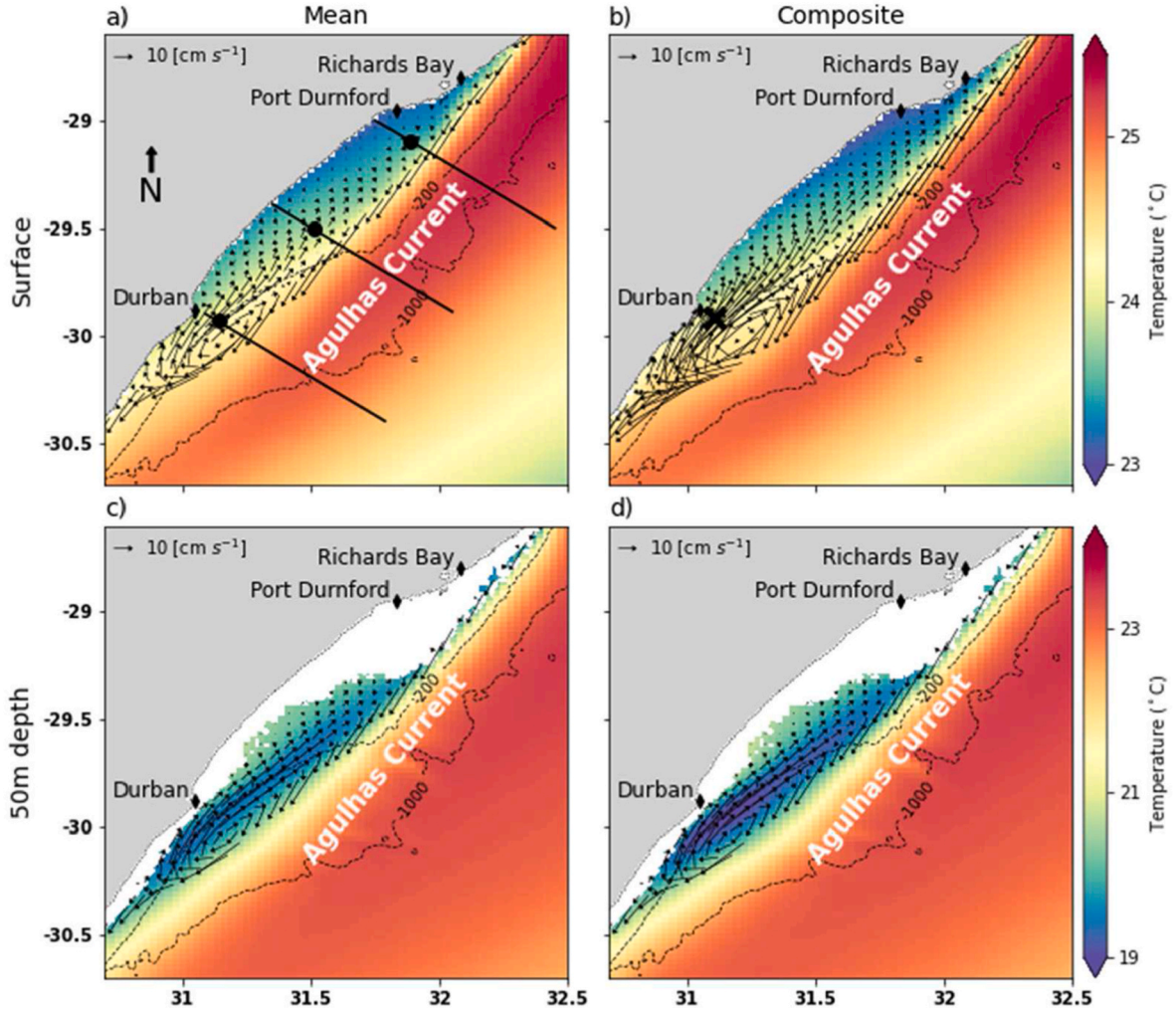


**Fig. 3.** Maps of the modelled circulation and water temperature, derived from January 2005 to December 2014. In (a) and (b), the respective time-averaged and north-eastward composite of the surface circulation is presented. The north-eastward composites include north-eastward velocities that exceed 10 cm/s at 31.11°E and 29.93°S, marked by the black cross in (b). Similarly (c) and (d), respectively, represent the mean and composite circulation and the water temperature at 50 m depth. Velocities are masked for currents off the shelf which exceed 30 cm/s in (a) and (c) and 50 cm/s in (b) and (d). These regions that do not show the direction of the circulation are associated with a south-westerly flow. The offshore grey lines are the 200 m and 1000 m isobaths and the three transect lines in (a) are later used for further analysis. The black dots along the transects in (a) mark the points that have the most frequent north-eastward flow along each transect. It must be noted that the temperature scales are different for the surface plots and the plots at depth.

the 50 m isobath) and an outer shelf (between the 50 m and 200 m isobath) region. The associated mean surface circulation patterns vary with the latitudinal position within these regions. In the northern KZN Bight, off Richards Bay (28.78°S; Fig. 3), the continental shelf is narrow and the mean surface circulation on the inner and outer shelves has a south-westward setting with an increased shoreward component near the coast. The outer shelf flow exceeds 100 cm/s and is much stronger than the inner shelf flow because it has a stronger Agulhas Current influence. Further south, the shelf widens as the coastline retracts, and from Port Durnford (28.92°S; Fig. 3), a north-eastward return flow can be observed on the mid-shelf in the mean and composite surface circulation. This flow is referred to as the NBC3 (Natal Bight Coastal Counter-Current). At the surface, the NBC3 is stronger in the composites compared to the overall mean surface circulation, while at depth not much difference is observed in the strength of the north-eastward flow.

The NBC3 dominates the outer shelf circulation in the southern KZN Bight. As it moves north towards Port Durnford, it propagates along the wide, inner shelf, crossing the isobaths to remain along a southwest-northeast axis and parallel to the coast. In the southern KZN Bight, the NBC3 is about 20 km wide and widens but weakens in the central KZN Bight. In the northern KZN Bight, it further weakens and becomes thinner to disappear roughly off Richards Bay (28.78°S, indicated in Fig. 3). Inshore of the NBC3, another coast-aligned, south-westward mean surface flow is present, which also stretches from Port Durnford over the central KZN Bight and reaches as far south as Durban. In the central KZN Bight, this current is about 10 km wide and therefore dominates the narrow central inner shelf surface circulation. It strengthens towards the south and its southern limit is marked by the cyclonic Durban Eddy, which extends from the coast onto the shelf break between 29.8°S and 30.2°S. The Durban Eddy results in strong mean north-eastward surface currents on the KZN Bight's shelf and marks the origin of the NBC3. In this region, the surface speeds of the NBC3 are fastest, with mean speeds exceeding 10 cm/s. Further north, the NBC3 rarely exceeds a mean surface flow of 5 cm/s.

The NBC3 is also clearly represented at 50 m depth. It transports cooler water onto the KZN Bight's shelf and has similar, but slightly reduced velocities here compared to the surface. The composite velocities are stronger and the water transported onto the shelf is cooler than in the mean circulation at depth. At the points marked along the transect lines in Fig. 3a, the surface north-eastward flow is observed 30% of the

time in the northern KZN Bight, 40% of the time in the central KZN Bight and 58% of the time in the southern KZN Bight. Therefore, a north-eastward flow is most common in the southern KZN Bight and its frequency decreases northwards.

### 3.2. The KZN Bight's mean vertical circulation

To complement the mean horizontal surface circulation and the circulation at 50 m depth presented in Fig. 3, mean vertical sections are plotted along the three transects marked in Fig. 3a. Along all the transects, the vertical sections present the south-westward flowing Agulhas Current as a feature that extends below 1000 m depth. It is strongest near the surface on the continental slope and its core, where south-westward flow is the strongest, follows the continental slope. Therefore, in the widened shelf region of the central KZN Bight, the Agulhas Current's core is further offshore (Fig. 3b). The vertical sections in Fig. 4 reveal that the NBC3, that was first observed by the drifter trajectories and later confirmed by the model's surface circulation, extends throughout the water column of the KZN Bight's shelf.

According to the 10-year model output, the shelf is thin and steep with a strong north-eastward current off Durban, which can exceed 20 cm/s at its core (Fig. 4c). This north-eastward flow has a width of roughly 15 km, which it maintains until a depth of 400 m. Thereafter it narrows, but at 800 m depth, it starts to widen and strengthen again. This is where Beal and Bryden (1997) describe the location of the Agulhas Undercurrent, which has matching features with the subsurface north-eastward current observed in the model. In the southern KZN Bight (Fig. 4c), the mean north-eastward transport in the top 600 m is 0.26 Sv and decreases northwards as the velocity and the vertical extent of the north-eastward flow decreases.

Further north, in the central KZN Bight (Fig. 4b), the shelf widens and becomes shallower, with depths not exceeding 100 m until over 30 km offshore. Against the coast, a weak surface south-westward flow is present in the top 10 m, which is only noticeable by the presence of the thick black line in Fig. 4b that marks the transition between a north-eastward and south-westward flow. However, this south-westward flow is not observed offshore of 10 km on the KZN Bight's shelf, where the mean vertical circulation is dominated by a north-eastward current that extends throughout the water column. This matches the findings of the mean surface circulation in Fig. 3. In the central KZN Bight, the north-eastward flow on the shelf exceeds 10 cm/s at its core and is, therefore, weaker than in the southern KZN Bight. It extends to 600 m depth and therefore has a deeper vertical extent compared to in the southern transect, but it is only observed as a very narrow seabed flow. Within the domain of the section presented in Fig. 4b, no other north-eastward flow at depth is observed in the central KZN Bight.

In the northern KZN Bight, near Port Durnford (28.92°S; Fig. 4a), the continental shelf is still wide and shallow, with water depths only exceeding 50 m, 30 km offshore. A mean north-eastward flow is again observed on the shelf and dominates most of the shelf circulation in the inshore 20 km. The northern KZN Bight's north-eastward flow is the weakest and does not exceed 5 cm/s. A very shallow, south-westward surface current in the inshore 10 km is also present, which can only be observed as a zero-velocity line in Fig. 4a because it is too shallow to be presented in the section. From 900 m depth, another very narrow and weak north-eastward flow is observed along the seafloor, which extends until 1200 m depth.

In summary, the model's mean vertical circulation captures the south-westward Agulhas Current as a deep and dominant feature on and offshore of the KZN Bight's shelf. In addition, it shows a north-eastward flow at depth on the shelf break, namely the Agulhas Undercurrent, together with another north-eastward flow that extends throughout the water column on the shelf: the Natal Bight Coastal Counter-Current (NBC3). The NBC3 is widest, deepest and strongest in the southern KZN Bight, where it can connect with the Agulhas Undercurrent. Inshore of the NBC3, a mean south-westward flow is also observed in the northern and central KZN Bight, but it is weaker and shallower than the NBC3.

### 3.3. Variability of the surface circulation in the core of the Natal Bight Coastal Counter-Current (NBC3)

Insight into the variability of the KZN Bight's surface circulation is gained using a timeseries of the alongshore currents off Durban, at the

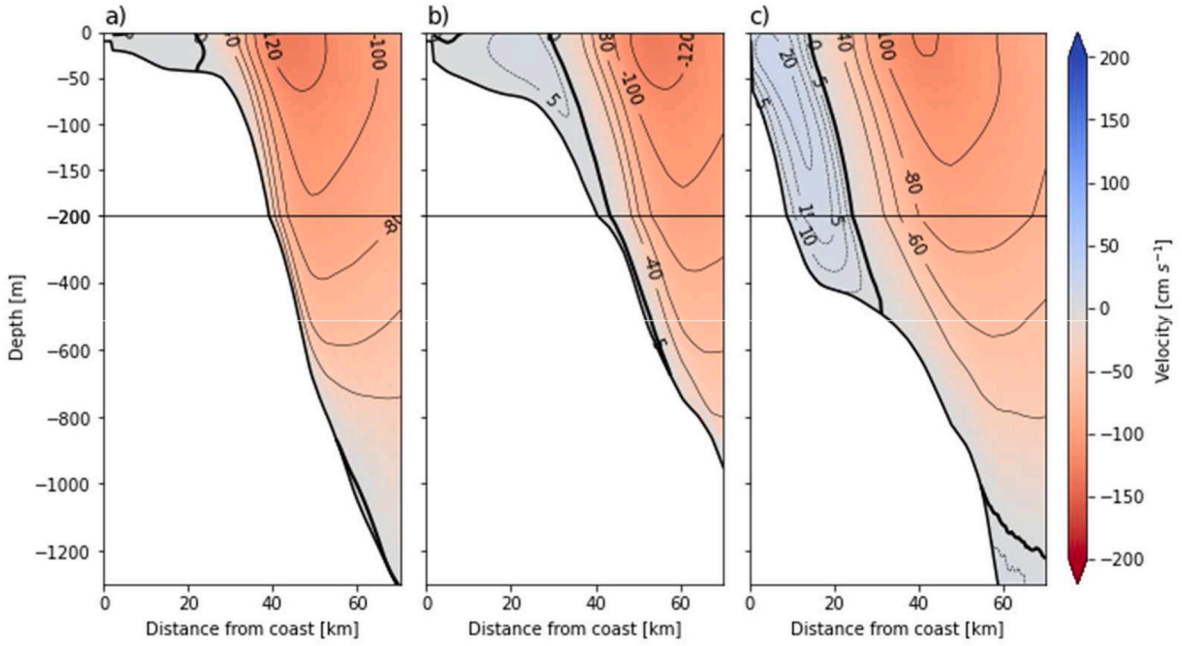


**Fig. 4.** Modelled vertical sections of the 10 year mean current velocities derived across the transects and presented in Fig. 3a. In (a), the northern transect is depicted, (b) shows the central transect and (c) represents the southern transect. The bold black lines are the transition lines between northward and southward velocities and the thinner solid black lines are the southward velocity contours, while the dotted thinner black lines are the northward velocity contours. A northward flow is positive and blue, while a southward flow is negative and marked with red.

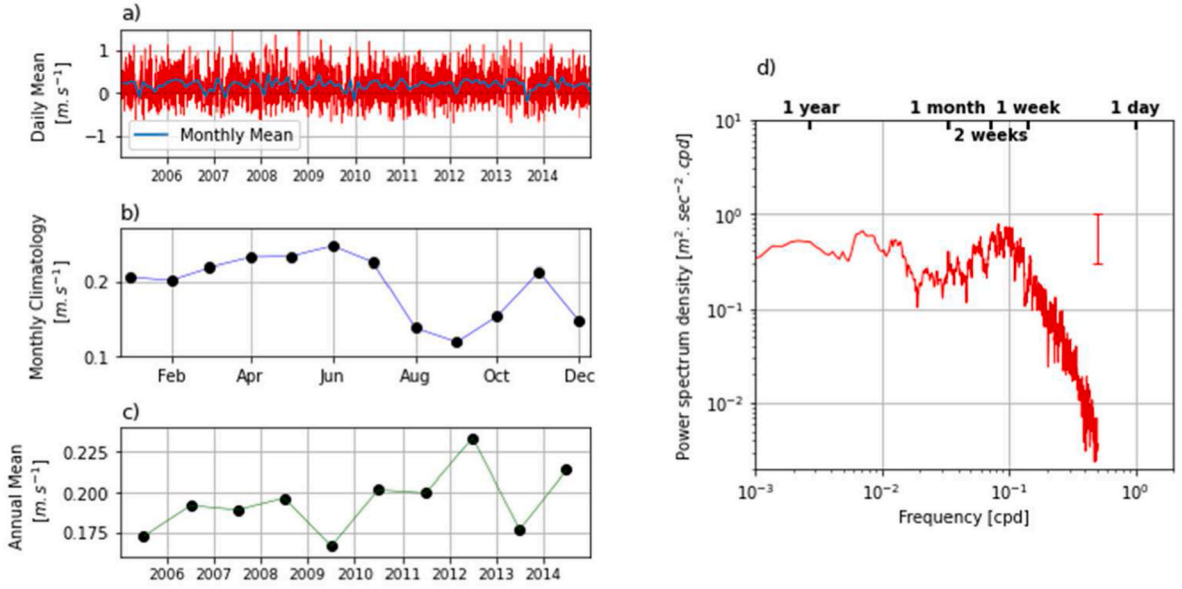


**Fig. 5.** Time-series of the (a) daily and monthly means, (b) monthly climatology and (c) annual means of the 10-year model surface circulation in the KZN Bight at the point with the strongest mean north-eastward shelf flow marked in Fig. 3b (31.11°E, 29.92°S). Currents are rotated −50° to display the alongshore circulation and the monthly means are superimposed on the daily mean figure. In (d), the power spectrum density of the total signal of the surface currents is presented, using the multitaper method. The error bar represents the 95% confidence interval of the signal and the frequency unit is cycles per day (cpd).

point of maximum mean north-eastward flow (31.11°E, 29.92°S and Fig. 3b). The time-series reveals that the circulation is highly variable with a standard deviation of 38 cm/s, which is stronger than the mean velocity of 20 cm/s. Alternating north-eastward and south-westward currents are observed on a daily to weekly timescale, with no clear pattern (Fig. 5a). The alongshore currents are, however, predominantly north-eastward with stronger velocities that may exceed 1.5 m/s on a daily average. This is in contrast to the occasionally observed south-westward flow, whose daily mean rarely exceeds 0.5 m/s during the investigated 10 years. The positive trend of 2 cm/s/10-years derived over the 10-year model output is statistically insignificant.

Overlayed onto the daily mean velocities in Fig. 5a, is the monthly mean. Monthly means show the ubiquitous presence of the NBC3, with only 7 instances of south-westerly flow detected over the 10-year period. The monthly climatology, obtained by averaging all monthly means, shows no clear seasonal cycle, but it does capture a weak NBC3 current strength reduction from August to December (Fig. 5b). At this location, each annual mean over the 10-year time-series has a north-eastward setting (Fig. 5c), with a strength ranging from 16 cm/s in 2009 to over 23 cm/s in 2012 and with an interannual standard deviation of 2 cm/s.

Fig. 5d shows the spectrum of along-shore surface current speeds off Durban, using a multitaper method (Babadi and Brown, 2014). This spectrum is relatively flat for periods larger than 100 days. It displays a small annual maximum, but according to the 95% confidence error bar, this peak is statistically insignificant. Another wide peak can be observed between 10 and 14 days, which is statistically significant and according to Guastella and Roberts (2016), corresponds to the typical period of the Durban Eddy life cycle (in absence of Natal Pulses).

### 3.4. Drivers of the circulation

Previous studies suggest that current variabilities on the KZN Bight's shelf are mostly driven by the Agulhas Current and the local winds. To further investigate this, the KZN Bight is divided into three transect lines presented in Fig. 3, which span across the northern, central and southern KZN Bight. The along- and across-shore surface current speeds are correlated to the Agulhas Current core's along- and across-shore surface current speeds for each transect and also to the local winds at the midpoint of each transect. Understanding the drivers of the overall circulation provides insight into the drivers of the north-eastward flow investigated in this study. The current correlations are visualised and presented in the left column of Fig. 6, while the wind and current correlations are presented in the right column of Fig. 6.

Naturally, the current correlations in the left column of Fig. 6 have a perfect correlation at the core of the Agulhas Current, as the remaining points along the transects are correlated to this core. In all the transects, across- and along-shore correlations decrease rapidly away from the Agulhas Current core and they usually decrease faster inshore of the current compared to offshore (Fig. 6a, c and 6e). Almost all the current correlations are statistically significant. The across-shore current correlations are always positive and are either equal to, or exceed, the alongshore correlations, which drop to negative values on the shelf, but increase again to near-zero values at the coast. A possible explanation for stronger across-shore correlations is that across-shore anomalies are associated with Agulhas Current meanders, increasing their correlation to the Agulhas Current core. Across-shore correlations on the shelf overall have the strongest positive correlations in the southern KZN Bight, as well as the strongest negative along-shore correlations of below −0.3, roughly 10 km offshore (Fig. 6e). This makes the southern KZN Bight overall the most predictable (Fig. 6).

Correlations between along-shore and across-shore winds and currents in the KZN Bight are overall positive but weak (Fig. 6b, d and 6f). They are particularly weak offshore of the 200 m isobath and on the continental slope, where the Agulhas Current is located (Fig. 3). In these regions, the across-shore correlations are mostly equal to, or close to zero and along-shore correlations do not exceed a correlation of 0.25. Most of the across-shore correlations offshore of the 200 m isobath are statistically insignificant, while the other correlations are all significant at the 95th percentile.

On the shelf, the correlations increase, where along-shore correlations exceed 0.5 in the northern (Fig. 6b) and central (Fig. 6d) transects. Across-shore components again have a lower correlation coefficient at every location along the transects, but also display a strong increase towards the coast, particularly inshore of the 50 m isobath. The across-

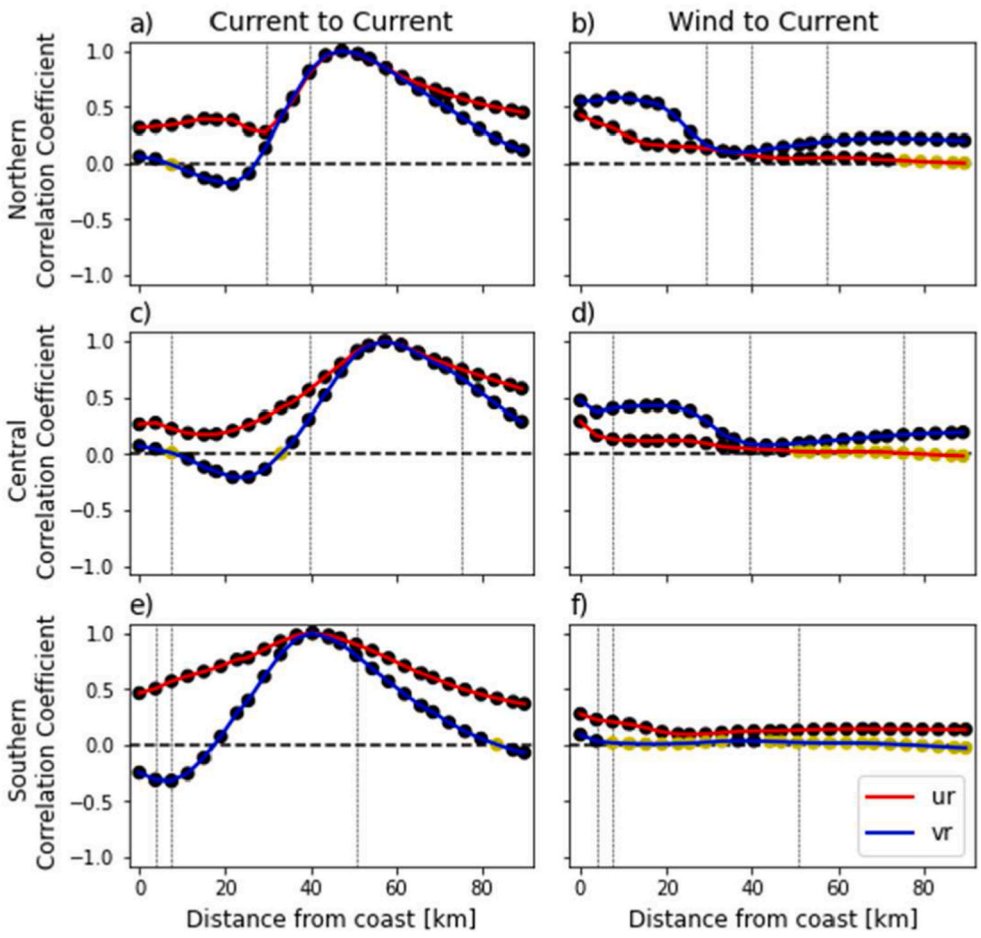


**Fig. 6.** The Pearson correlation coefficient of the surface circulation at the Agulhas Current core and remaining points along the (a) northern, (c) central and (e) southern KZN Bight transects from Fig. 3a, as well as the Pearson correlation coefficients of wind and surface currents along the (b) northern, (d) central and (f) southern transects. The red lines are the across-shore components (ur) and the blue lines show along-shore components (vr) of the correlations. The vertical black dotted lines indicate the location of the 50 m, 200 m and 1000 m isobaths. Black dots indicate correlations significant at the 95th percentile, while the remaining correlations are plotted using yellow dots.

shore correlations are strongest in the northern KZN Bight, where they almost reach a correlation of 0.5 at the coast. In the southern KZN Bight (Fig. 6f), the along-shore and across-shore correlations are the weakest and only show some correlation at the most coastal transect point. Therefore, the wind and surface currents correlate mostly on the shelf of the northern and southern KZN Bight and otherwise do not have a strong correlation. Their strongest correlations are often within the shelf regions that have lower current correlations in Fig. 6. To investigate if the correlations had a lag effect, we tested the lagged correlation, but for the current - current as well as the wind-current correlations, no difference was observed.

### 3.5. Impact of the circulation on MPA connectivity

Virtual particles were released in four MPAs along the KwaZulu-Natal coastline to understand the impact of the Natal Bight Coastal Counter-Current (NBC3) on the connectivity of Marine Protected Areas (MPAs) and on the surface dispersion. They were released during the three strongest northward and the three strongest southward surface flow events that were observed at the 50 m isobath throughout all three KZN Bight transects. These events were identified as three large peaks, northward flows, and three large troughs, southward flows, in the time-series of the KZN Bight's along-shore surface currents. The 50 m isobath was chosen for each transect, because it forms part of the mean northward flow observed in the mean circulation in Fig. 3. The percentage of virtual particles entering each MPA was calculated and is provided in Fig. 7, along with the average age and average residence time within each MPA. The age represents the travel time of the virtual particles following their release, while the residence time represents the time that virtual particles spent within each MPA. These two parameters together provide an indication of the extent of the local water retention and can be used to indicate how quickly virtual particles leave the KZN Bight system and how long they stay within a MPA.

When virtual particles were released in iSimangaliso during northward events corresponding to NBC3 events, 70% on average entered Protea Banks, while the least number of virtual particles, only 38% on average, entered uThukela Banks (Fig. 7a). Therefore, many virtual particles released in iSimangaliso skipped uThukela Banks and Aliwal Shoal to only enter the southernmost Protea Banks MPA. In contrast, during southward KZN Bight events, on average almost half of the virtual particles released in iSimangaliso entered uThukela Banks, while the least number of virtual particles, 19% on average, entered Aliwal Shoal. This is because some of the virtual particles were either trapped in uThukela Banks and did not continue to move downstream or they skipped Aliwal Shoal as they moved downstream. Virtual particles released in iSimangaliso have a similar average residence time, not exceeding 4 days within this MPA during northward and southward KZN Bight events. However, when the virtual particles enter uThukela Banks, their average residence time is longer during a northward surface flow (6.6 days) compared to a southward surface flow (2.8 days). The average residence time of virtual particles released in iSimangaliso is similar (roughly 1 day) at Aliwal Shoal and Protea Banks, during both northward and southward events. In a southward surface flow, the average age of virtual particles increases from iSimangaliso (5.4 days) southwards to Protea Banks (12.5 days). During the northward events, the average age is similar in iSimangaliso, but instead of increasing southwards, it is highest in uThukela Banks (13.4 days). This shows that the NBC3 promotes retention in uThukela Banks.

When virtual particles were released in uThukela Banks, neither the northward nor the southward surface flows carried any of these virtual

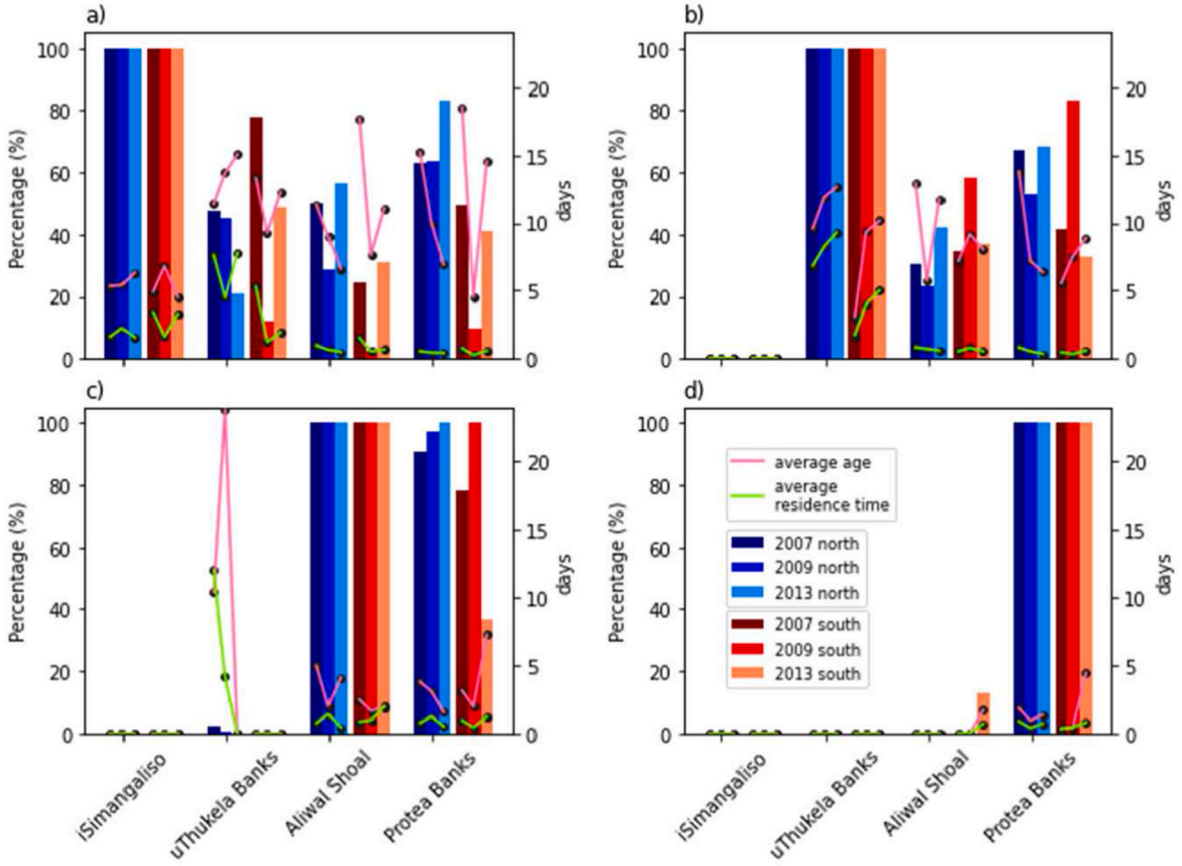


**Fig. 7.** The average residence time (green lines) and the average age (pink lines) of virtual particles released in the (a) iSimangaliso, (b) uThukela Banks, (c) Aliwal Shoal and (d) Protea Banks Marine Protected Areas (MPAs). Within the KZN Bight, three northward surface flow events during 2007, 2009 and 2013 are indicated by the blue bars, while three southward surface flow events during the same years are indicated by red bars. The height of the bars indicates the percentage of virtual particles that enter each MPA, in each case.

particles north into iSimangaliso (Fig. 7b). On average 63% and 53%, respectively, entered Protea Banks during northward and southward surface flows, while 32% and 43%, respectively, entered Aliwal Shoal. Therefore, during all the events, a large portion of virtual particles released in uThukela Banks skipped Aliwal Shoal but

entered Protea Bank further south. During the northward events, the average residence time for the virtual particles is the highest in uThukela Banks (8.1 days) and less than half during southward events (3.6 days). In Aliwal Shoal and Protea Banks, the average residence times of virtual particle released at uThukela Banks are similar and lowest during either circulation, never exceeding 1 day. Investigating the average ages reveals that uThukela Banks also has the highest average age of virtual particles during a northward surface flow (11.4 days). This again indicates that the NBC3 promotes retention in uThukela Banks. The average age decreases southwards during northward flows and reaches 9.1 days in Protea Banks. During a southward surface flow, the average age for virtual particles released in uThukela Banks is greatest in Aliwal Shoal (8.1 days), followed by uThukela Banks (7.5 days) and Protea Banks (7.3 days). Therefore, even with a southward flow, the retention of virtual particles is strongest in uThukela Banks, which could partly be explained by the larger size of uThukela Banks, which inflates the residence times.

Virtual particles released in Aliwal Shoal during these same events did not enter iSimangaliso, but 1% reached uThukela Banks during two of the northward events (Fig. 7c). These virtual particles had an average residence time of 8.1 days within this MPA and an average age of 17.1 days. None of the southward events advected virtual particles into uThukela Banks. Of the virtual particles released in Aliwal Shoal, 96% and 72% entered Protea Banks during northward and southward events, respectively. The average residence time rarely exceeded 1 day within any of the remaining events and the average age was roughly 4 days. Therefore, virtual particles overall spend little time in the two southernmost MPAs.

Virtual particles released in Protea Banks again neither entered iSimangaliso nor uThukela Banks (Fig. 7d). They only propagated into Aliwal Shoal during one southward flow event (2013) and at a very low level (4%). With 0.7 and 1.7 days, respectively, the average residence time and the average age was largest in Aliwal Shoal during the southward KZN Bight events that advected virtual particles into Aliwal Shoal. In Protea Banks, the average residence times and the average ages of virtual particles were very similar during either surface flow regime.

Overall, the largest percentage of virtual particles released in any MPA entered Protea Banks, where their residence times were short. Residence times in Aliwal Shoal and in iSimangaliso were of similar duration, while virtual particles in uThukela Banks had the highest residence times, particularly during a northward flow event. This indicates that the water retention is strongest within uThukela Banks. Virtual particles were not often advected north of the MPA in which they are released, only moving north of Aliwal Shoal and Protea Banks, respectively, during two northward events and one southward event. The average age of virtual particles usually increased southwards, but when virtual particles were advected north, the average ages in the northern MPAs were inflated due to the increased travelling times of the northward advected virtual particles.

## 4. Discussion

### 4.1. The circulation

Our model shows that the surface circulation of the KZN Bight's shelf is weak and variable, while it is strong with a south-westward setting on the shelf break, enforced by the Agulhas Current (Fig. 3). This is in agreement with Guastella and Roberts (2016) and Roberts et al. (2016). Prevailing surface circulation features previously identified and described on the shelf include the semi-permanent cyclonic Durban Eddy offshore and south of Durban (Roberts et al., 2016; Guastella and Roberts, 2016); the swirl circulation north of Durban, which has a northern boundary by the Tugela River mouth (Roberts et al., 2016); and the weak and variable alongshore currents in the northern KZN Bight (Schumann, 1981; Roberts et al., 2016; Roberts and Nieuwenhuys, 2016). Roberts et al. (2016) suggest that these features make up the mean surface circulation within the KZN Bight. At depth, another circulation feature is observed, known as the Agulhas Undercurrent, which is located along the continental slope, below the Agulhas Current and is most prominent at a depth of 1500 m, with a mean north-eastward velocity of 10 cm/s (Beal and Bryden, 1997; Beal, 2009). All these previously reported features are well characterized in our model's mean surface circulation (Fig. 3), its mean vertical circulation (Fig. 4) and in its time-series (Fig. 5). A simplified sketch of the mean circulation is presented in Fig. 8.

Even though several studies have focused on the KZN Bight's circulation, most of the previous research is based on time-limited, *in situ* observations, limiting the understanding of the mean surface circulation and its drivers. The most comprehensive depiction of the shelf circulation is based on the study by Roberts et al. (2016). They used four S-ADCP surveys in June 2005, September 2007, March 2009 and July 2010, which collected data over two to eight days. Satellite data was used to describe the KZN Bight's circulation during these S-ADCP surveys and they investigated the trajectories of satellite-tracked surface drifters deployed between April and August in 2010. Even though together, the data capture prominent circulation features, the only provide a brief insight from which no mean or seasonal patterns can be derived.

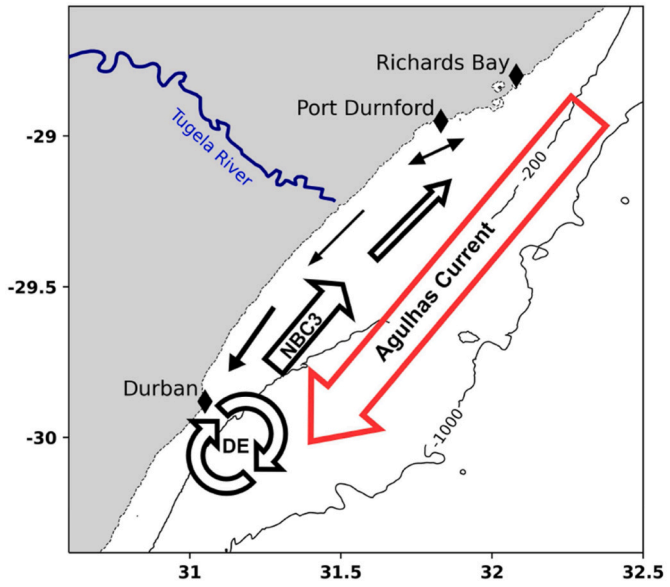


**Fig. 8.** A simplified diagram of the mean surface circulation in the KZN Bight. It presents the strong, offshore south-westward Agulhas Current, the Durban Eddy (marked 'DE'), the Natal Bight Coastal Counter Current (NBC3), the variable northern KZN Bight coastal currents and the mean coastal south-westward flow. Arrow thicknesses are roughly proportional to the strength of the flow that they represent.

The CROCO-WOES36 model applied in this study provides temporal and spatial coherence, which identifies links and fills gaps to provide an in-depth understanding of the surface flow, with a particular focus on the Natal Bight Coastal Counter-Current (NBC3). The model's mean surface flow matches the mean circulation features recently summarized by Roberts et al. (2016), i.e., the Agulhas Current along the shelf edge, the weak shelf currents and the Durban Eddy (Fig. 3). The model reveals that the NBC3 originates along the inshore edge of the Durban Eddy from where it extends north onto the KZN Bight's shelf (Fig. 3). On the shelf, the NBC3 then forms the inshore edge of another, weaker cyclonic feature north of the Durban Eddy, previously identified as the swirl circulation. The offshore edge of the swirl is also forced by the south-westward Agulhas Current and according to Roberts et al. (2016), it may eventually move downstream to replace preceding Durban Eddies. Inshore of the NBC3, the mean model output also reveals a coastal south-westward current along the inner shelf of the KZN Bight. This flow is occasionally reflected in the S-ADCP data from Roberts et al. (2016). At depth, the model displays the deeply extending Agulhas Current and the Agulhas Undercurrent with its core below 1300 m depth and a mean speed matching the findings of Beal and Bryden (1997) and Beal (2009).

The NBC3 identified by the coherent model output can also been observed in the trajectories of the *in situ* surface drifters (Fig. 2). River plumes visible in satellite imagery also provide evidence of a north-eastward flow across the KZN Bight. One recent example of such a north-eastward flow can be observed in a false colour image over the region, acquired on 14 April 2022 (https://odl.bzh/ATgKpRbM). Similarly, prawn larvae spawned in uThukela Bank at depths between 20 and 50 m also have been found to end up in Richards Bay and St Lucia estuarine nursery areas (Forbes and Cyrus, 1991), suggesting that the NBC3 is physically feasible and biologically probable to exists throughout the KZN Bight and may extend even further north. As it moves northwards across the KZN Bight's mid-shelf, the NBC3 weakens and becomes less frequent until it disappears off Richards Bay. In the transect along the southern KZN Bight, the NBC3's north-eastward flow is the most frequent, occurring 58% of the time in the 10-year model output. This matches the findings of Guastella and Roberts (2016), who observe a Durban Eddy in this region with its associated north-eastward flow in 55% of their data. In the central KZN Bight transect, the NBC3 is less commonly observed and in the northern KZN Bight, it is the least frequent and only occurs in 30% of the 10-year model output. This is because not every Durban Eddy may be equally strong to result in an equal NBC3 extent. Guastella and Roberts (2016) confirm that there is great variability between different Durban Eddies. The mean vertical structure also shows that the NBC3 is the strongest within the Durban Eddy (Fig. 4), also indicating that this feature is often the driver of a north-eastward flow on the shelf. Within the Durban Eddy, the NBC3 extends to depths below 400 m, almost connecting to the Agulhas Undercurrent (Fig. 4). Further north, it still extends throughout the water column on the shelf, but it remains on the shelf which becomes shallower northwards, meaning that the vertical extent of the NBC3 also decreases towards the north.

The time-series of the currents in the southern KZN Bight reveals that the circulation is highly variable with alternating north-eastward and south-westward surface currents (Fig. 5a). North-eastward flows are associated with Durban Eddies, while south-westward flows are likely linked to passing mesoscale perturbations associated with meanders in the Agulhas Current (Lutjeharms and Roberts, 1988; de Ruijter et al., 1999), as these break the Durban Eddies off their semi-permanent position (Guastella and Roberts, 2016). Tedesco et al. (2019) confirmed that such Natal Pulses are well presented in the CROCO model. The alternating currents within the model's Durban Eddy have no distinct trend or annual cycle, matching previous observations of the Durban Eddy frequency (Guastella and Roberts, 2016). In the spectral plot of Fig. 5d, a significant cycle with a frequency between 10 days and two weeks is observed. This is also in correspondence with the observations

from Guastella and Roberts (2016), who noted that Durban Eddies are observed for 8.4 days on average and the average time between events is 4.3 days when no Natal Pulses are observed. These cycles may be linked to atmospheric variabilities, as observed in the adjacent Benguela current (Nelson and Hutchings, 1983). However, the point within the Durban Eddy chosen for the spectral plot has a low wind-current correlation in Fig. 6 as it is strongly eddy-driven and may therefore not have much of an atmospheric origin.

A weak and insignificant seasonal cycle is also observed in the source region of the NBC3, within the Durban Eddy, with a generally stronger NBC3 in austral autumn (March to June) (Fig. 5b). Although it is notoriously difficult to model the seasonality in Agulhas Current transport, this CROCO simulation captures a large part of the signal (Hutchinson et al., 2018, Fi.g. 12). Krug and Tournadre (2012) observed a stronger Agulhas Current in austral summer (December to March) and similarly, a seasonal cycle was also observed by Beal and Elipot (2016), but both studies observed this seasonal cycle at a much higher latitude. When the Agulhas Current is stable, the Durban Eddy is present and drives a north-eastward shelf flow, but when Natal Pulses occur in the current, they result in a breaking off and southward escaping Durban Eddy, which in turn results in a south-westward surface shelf flow (Guastella and Roberts, 2016). Therefore, the Agulhas Current is likely linked to the Durban Eddy and a seasonal cycle in the current may drive a weak seasonal cycle in the Durban Eddy, observed in the spectral plot of Fig. 5.

The instantaneous and linear negative correlations between the offshore Agulhas Current and the shelf circulation also indicate a relationship between the Agulhas Current and the Durban Eddy, as the southern KZN Bight is the most predictable with the strongest alongshore correlations between the Agulhas Current and the shelf currents (Fig. 6). Coastal western boundary countercurrents described in the western flank of the Florida Current (Soloviev et al., 2017) and in the Kuroshio Current (Hsu et al., 2018) also suggest drivers from the offshore western boundary currents. More specifically, they respectively explain the countercurrent of the Florida Current by an alongshore pressure gradient force as well as wind stress and the Kuroshio countercurrent by the occurrence of a cold dome and a wind-driven current. Bane and Dewar (1988) also notice a semi-permanent gyre in the South Atlantic Bight, which similarly may result in an equatorward shelf break flow also observed by Lee et al. (1991). Even in the Guinea Current, which is however not a western boundary current, a coastal countercurrent is occasionally observed. Lemasson and Rebert (1968) suggest it is the Ivoirian Undercurrent, which may surface when the Guinea Current moves offshore. However, both Ingham (1970) and Djakouré et al. (2014) suggest it is driven by cyclonic eddies, similar to the Durban Eddy in the KZN Bight.

North of the Durban Eddy, the current correlations decrease, as other drivers become more persistent. Even at the source of the NBC3 in the southern KZN Bight, alternating north-eastward and south-westward currents are observed on the KZN Bight's shelf that occur too frequently to be accounted for by the perturbations in the Agulhas Current front (Fig. 5). The instantaneous, linear correlations between the surface currents and the near-surface wind reanalyses show that almost no correlation is observed on the shelf break where the Agulhas Current is located, but the correlations increase inshore (Fig. 6). Correlations are particularly strong in shallow and coastal regions, such as in the northern KZN Bight, where they can exceed values of 0.5. This matches the previous observations of Roberts et al. (2016) who suggest that local winds strongly influence the surface circulation within the KZN Bight, with a particularly strong relationship in the northern KZN Bight. Winds therefore also partially drive the NBC3 located in this region and this matches results from (Hsu et al., 2018), who suggest a wind influence on the coastal western boundary countercurrent observed in the Kuroshio Current. In this region, the south-westerly monsoons create a wind-driven current in the Taiwan Strait, which enforces the surface countercurrent.

### 4.2. Impact of the NBC3 on retention and MPA connectivity

The reproductive success of many important fish species relies on the ocean's circulation, as this affects the dispersion of their larvae and their survival success. The KZN Bight has previously been identified as an important nursery and spawning ground (Hutchings et al., 2002), which means that larvae are released into the circulation within this region. Due to their small size and complex behaviour, it is difficult to track larvae directly (Leis, 2006; North et al., 2008) and therefore this study tracks virtual particles representing passively drifting larvae in the model. They are released at the surface in a range of Marine Protected Areas (MPAs), which were established to protect vulnerable species and habitats such as the KZN Bight. By releasing and tracking virtual larvae, the extent to which these MPAs are connected during different circulations regimes can be better quantified. Therefore, virtual particles are released in the presence or absence of the NBC3, to determine its impact on MPA connectivity along the KwaZulu-Natal coastline.

The virtual trajectories reveal a strong southward MPA connectivity between iSimangaliso, uThukela Banks, Aliwal Shoal and Protea Banks, which is driven by the Agulhas Current. The Agulhas Current shortens the average residence time of virtual particles in these MPAs, particularly within Aliwal Shoal and Protea Banks (Fig. 7). ISimangaliso is the largest MPA investigated, which inflates its average residence time in this region. However, these residence times are still shorter than the average residence time of virtual particles within uThukela Banks, a sheltered region due to its widened shelf that decreases the Agulhas Current influence. The Agulhas Current offshore of uThukela Banks transports less virtual particles onto the KZN Bight's shelf when a NBC3 is present (Fig. 7). Therefore, passively floating larvae would ideally need to be spawned within the KZN Bight to remain trapped on the shelf, instead of having a northern or offshore origin. When they do enter uThukela Banks, virtual particles are either pushed onto the northern shelf by the inshore edge of the Agulhas Current or they are pulled out of the current and into uThukela Banks by the Durban Eddy.

Out of all the investigated MPAs, the NBC3 has the largest influence on uThukela Banks. The average residence times when the NBC3 is present are almost double those of virtual particles during southward events, while not much difference is observed in the other MPAs (Fig. 7). This is also indicated by the drifter in Fig. 2b, which is trapped in uThukela Banks for a few days before it escapes the region. Average particle ages in uThukela Banks are also greater when the NBC3 and the Durban Eddy are present (Fig. 7). The trajectories show that virtual particles leaving iSimangaliso are likely to enter uThukela Banks via the Durban Eddy during the NBC3 event, which is a longer path and increases their age as they enter uThukela Banks. Virtual particles entering uThukela Banks from the northern KZN Bight during southward events, where the Agulhas Current pushes them onto the shelf, have a shorter path and are therefore younger as they enter. Virtual particles that leave and re-enter a MPA may also inflate the average age in uThukela Banks. Larger ages have implications for the recruitment viability as species with longer larval competence times could still be viable or ready to settle in the MPAs that they pass at a later stage.

The mean circulation shows little evidence of the NBC3 north of Richards Bay and therefore the NBC3 does, on average, not reach iSimangaliso to create a northward connection between it and uThukela Banks (Fig. 7). However, prawn larvae spawned in Thukela Bank at depths between 20 and 50 m have been found to end up in Richards Bay and even in St Lucia estuarine nursery areas (Forbes and Cyrus, 1991), which proves that occasionally the NBC3 can reach these regions while transporting suspended larvae. Similarly, the drifter in Fig. 2c indicates an event of a north-eastward shelf flow that pushes the drifter into the southern section of iSimangaliso, where it beaches. South of the KZN Bight, virtual particles may be transported from Aliwal Shoal north into uThukela Banks when the Durban Eddy and its associated NBC3 extends into Aliwal to connect these two MPAs (Fig. 7). This is demonstrated by the drifter in Fig. 2a. Further south, inshore eddies associated with

meanders in the Agulhas Current may also result in northward shelf currents (Lamont et al., 2021), which can increase the connectivity and average age northwards between Protea Banks and Aliwal Shoal, as observed in Fig. 7.

Larvae do not only require a sheltered region to maximise their survival success, but they also rely on nutrient availability. When oligotrophic Agulhas Current water is transported onto the southern KZN Bight's shelf along the outer edge of the Durban Eddy, or by the swirl (Meyer et al., 2002; Roberts et al., 2016), it may decrease nutrient concentrations in the KZN Bight. Since the NBC3 originates within the Durban Eddy and forms the inshore edge of the swirl further north, it may equally be associated with nutrient-poor water. However, usually the Durban Eddy, and therefore the NBC3, are associated with upwelling and increased nutrients as well as productivity on the shelf (Roberts et al., 2010). Due to its extent and orientation, the NBC3 may also trap riverine nutrients along the coast by preventing an offshore loss (Fig. 3). This would also increase local nutrients on the KZN Bight's shelf and further favour nursery and spawning conditions, as have been suggested by Hutchings et al. (2002). In summary, the NBC3 is most likely associated with favourable conditions for recruitment. Another source of nutrients to the shelf is coastal and shelf-edge upwelling in the northern KZN Bight (Roberts and Nieuwenhuys, 2016), which is partly wind-driven and supported by stronger wind-current correlations in the northern KZN Bight (Fig. 6).

Marine ecosystems depend on the ocean's circulation, which forms more favourable conditions for recruitment when a NBC3 (and therefore a Durban Eddy) is present, as it increases nutrients and water retention. Meanders in the Agulhas Current disrupt the circulation and increase the offshore loss of passively drifting larvae from the KZN Bight's shelf and therefore uThukela Banks. Future studies could allow the virtual particles to sink. This would allow tracking their vertical profiles and disregarding those that sink too deep for larval survival, making the experiments more realistic. Similarly, considering appropriate swimming behaviours for their trajectories and releasing virtual particles during spawning seasons on their spawning grounds, with due consideration of larval competency periods, would also provide more accurate insight into their trajectories and likely survival within recruitment areas.

## 5. Conclusion

The KwaZulu-Natal (KZN) Bight is a small coastal region along Africa's south-east coast. Large knowledge gaps are present in the understanding of its circulation, as previous studies mostly focus on spatially and temporally limited data that usually only provide insight into the surface circulation. With the help of model output from the 3D CROCO-WOES36 configuration for the region, the KZN Bight's circulation is further studied and it has revealed a newly identified circulation feature, referred to as the Natal Bight Coastal Counter-Current (NBC3). Coastal western boundary countercurrents are also described in the Florida (Soloviev et al., 2017) and Kuroshio Currents (Hsu et al., 2018), where they are similarly driven by pressure gradients and wind stress.

The NBC3 originates in the southern KZN Bight, on the inshore edge of the cyclonic Durban Eddy. In this region, the NBC3 is observed in almost 60% of the 10-year model output and is about 20 km wide. It has a deep vertical extent, reaching past the continental slope and almost connecting to the Agulhas Undercurrent, a subsurface return flow that opposes the Agulhas Current. As the NBC3 moves north onto the KZN Bight's shelf, it becomes the inshore edge of another cyclonic circulation feature on the continental shelf, the 'swirl' circulation. The NBC3 moves parallel to the coast while weakening and becoming less frequent northwards until it is only present in 30% of the output in the northern KZN Bight. Following the shape of the KZN Bight's shelf, the NBC3 reaches its maximum width in the central KZN Bight and narrows northwards until it eventually disappears roughly 190 km from its origin. On the wide shelf of the KZN Bight, the NBC3 does not reach the continental slope, but it does extend throughout the shelf's water column. When anticyclonic eddies offshore of the Agulhas Current propagate southwards, the current shear between the shelf and offshore currents weakens and the Durban Eddy breaks off from its semi-permanent position. As a result, the NBC3 is periodically replaced by a south-westward shelf flow during these events.

The Agulhas Current and near-surface winds are correlated to the shelf currents to investigate the drivers of the circulation. Winds drive daily to weekly north-south alternations in the shelf currents, while perturbations along the Agulhas Current front have a longer timescale of around two weeks. In the shallow northern KZN Bight, the correlation between winds and surface currents are strong, particularly along the coast. The central KZN Bight also has a strong coastal correlation to local winds, while the southern KZN Bight has very little wind influence. This region is mostly driven by the Agulhas Current. When the Agulhas Current is stable and strongest near the continental slope, the current shear towards the slow shelf currents is strongest and the Durban Eddy with its inshore north-eastward flow is formed, explaining the strong negative correlations.

The impact of the NBC3 on the connectivity of local Marine Protected Areas (MPAs) is investigated using virtual particle tracking tools. Virtual particles are released in surrounding MPAs during multiple NBC3 as well as southward surface currents within the KZN Bight. Overall, the NBC3 mostly influences uThukela Banks, located on the KZN Bight's shelf, increasing residence times. The NBC3 does not seem to impact MPAs north of uThukela Banks, but may increase the connectivity of southern and mid-KZN Bight MPAs, when its origin, the Durban Eddy, is far enough south. By increasing the residence times within uThukela Banks, the NBC3 has a strong impact on the local biology of the KZN Bight, which is known to be an important nursery and spawning ground due to its nutrient inputs and shelter from the Agulhas Current.

## Declaration of competing interest

The authors declare that they have no known competing financial interests or personal relationships that could have appeared to influence the work reported in this paper.

## Acknowledgements

This work was granted access to the HPC resources of IDRIS under the allocation A0040107630 made by GENCI in Paris, France. The coastal drifter datasets were supplied by the DSI/NRF/ACEP Captor Project (Grant 110763) and the CROCO model data is available at http://dap.saeon. ac.za/thredds/catalog/SAEON.EGAGASINI/2019. Penven/DAILY_MEANS/1_36_degree/catalog.html. This work is supported by the National Research Foundation, the Nansen-Tutu Center, as well as by ISblue project, Interdisciplinary graduate school for the blue planet (ANR17-EURE-0015) and co-funded by a grant from the French government under the program "Investissements d'Avenir".

## References

Andrello, M., Guilhaumon, F., Albouy, C., Parravicini, V., Scholtens, J., Verley, P., Barange, M., Sumaila, U.R., Manel, S., Mouillot, D., 2017. Global mismatch between fishing dependency and larval supply from marine reserves. Nat. Commun. 8, 1–9.

Archer, M.R., Roughan, M., Keating, S.R., Schaeffer, A., 2017. On the variability of the East Australian Current: jet structure, meandering, and influence on shelf circulation. J. Geophys. Res.: Oceans 122, 8464–8481.

Babadi, B., Brown, E.N., 2014. A review of multitaper spectral analysis. IEEE (Inst. Electr. Electron. Eng.) Trans. Biomed. Eng. 61, 1555–1564.

Bane, J.M., Dewar, W.K., 1988. Gulf Stream bimodality and variability downstream of the charleston bump. J. Geophys. Res.: Oceans 93, 6695–6710.

Barlow, R., Kyewalyanga, M., Sessions, H., Van den Berg, M., Morris, T., 2008. Phytoplankton pigments, functional types, and absorption properties in the Delagoa and Natal Bights of the Agulhas ecosystem. Estuarine. Coast. Shelf Sci. 80, 201–211.

Beal, L.M., 2009. A time series of Agulhas Undercurrent transport. J. Phys. Oceanogr. 39, 2436–2450.

Beal, L.M., Bryden, H.L., 1997. Observations of an Agulhas undercurrent. Deep Sea Res. Oceanogr. Res. Pap. 44, 1715–1724.

Beal, L.M., Elipot, S., 2016. Broadening not strengthening of the Agulhas Current since the early 1990s. Nature 540, 570–573.
Beal, L.M., Elipot, S., Houk, A., Leber, G.M., 2015. Capturing the transport variability of a western boundary jet: results from the Agulhas current time-series experiment (ACT). J. Phys. Oceanogr. 45, 1302–1324.
Beckley, L., Hewitson, J., 1994. Distribution and abundance of clupeoid larvae along the east coast of South Africa in 1990/91. S. Afr. J. Mar. Sci. 14, 205–212.
Carter, R.A., Schleyer, M.H., 1992. Plankton Distributions in Natal Coastal Waters. Coastal and Estuarine.
CROCO. Coastal and Regional Ocean COmmunity model, 2022-08- 16. https://www.croco-ocean.org/.
Da Silveira, I., Lima, J., Schmidt, A., Ceccopieri, W., Sartori, A., Franscisco, C., Fontes, R., 2008. Is the meander growth in the Brazil Current system off Southeast Brazil due to baroclinic instability? Dynam. Atmos. Oceans 45, 187–207.
de Ruijter, W.P., Van Leeuwen, P.J., Lutjeharms, J.R., 1999. Generation and evolution of natal Pulses: solitary meanders in the Agulhas current. J. Phys. Oceanogr. 29, 3043–3055.
Debreu, L., Marchesiello, P., Penven, P., Cambon, G., 2012. Two-way nesting in split-explicit ocean models: algorithms, implementation and validation. Ocean Model. 49, 1–21.
Dee, D.P., Uppala, S.M., Simmons, A.J., Berrisford, P., Poli, P., Kobayashi, S., Andrae, U., Balmaseda, M., Balsamo, G., Bauer, d.P., et al., 2011. The ERA-Interim reanalysis: configuration and performance of the data assimilation system. Q. J. Roy. Meteorol. Soc. 137, 553–597.
Delandmeter, P., Sebille, E.v., 2019. The Parcels v2. 0 Lagrangian framework: new field interpolation schemes. Geosci. Model Dev. (GMD) 12, 3571–3584.
Djakouré, S., Penven, P., Bourlès, B., Veitch, J., Koné, V., 2014. Coastally trapped eddies in the north of the Gulf of Guinea. J. Geophys. Res.: Oceans 119, 6805–6819.
Elipot, S., Beal, L.M., 2015. Characteristics, energetics, and origins of Agulhas Current meanders and their limited influence on ring shedding. J. Phys. Oceanogr. 45, 2294–2314.
Ferry, N., Parent, L., Garric, G., Bricaud, C., Testut, C., Le Galloudec, O., Lellouche, J., Drevillon, M., Greiner, E., Barnier, B., et al., 2012. GLORYS2V1 global ocean reanalysis of the altimetric era (1992–2009) at meso scale. Mercator Ocean–Quaterly Newslett. 44.
Forbes, A., Cyrus, D., 1991. Recruitment and origin of penaeid prawn postlarvae in two south-east African estuaries. Estuar. Coast Shelf Sci. 33, 281–289.
Green, A., MacKay, C., 2016. Unconsolidated sediment distribution patterns in the KwaZulu-Natal Bight, South Africa: the role of wave ravinement in separating relict versus active sediment populations. Afr. J. Mar. Sci. 38, S65–S74.
Gründlingh, M., 1974. A description of inshore current reversals off Richards Bay based on airborne radiation thermometry. In: Deep Sea Research and Oceanographic Abstracts. Elsevier, pp. 47–55.
Guastella, L., Roberts, M., 2016. Dynamics and role of the Durban cyclonic eddy in the KwaZulu-Natal Bight ecosystem. Afr. J. Mar. Sci. 38, S23–S42.
Gula, J., Molemaker, M.J., McWilliams, J.C., 2015. Gulf Stream dynamics along the southeastern US seaboard. J. Phys. Oceanogr. 45, 690–715.
Hart-Davis, M., Backeberg, B., 2021. Towards a particle trajectory modelling approach in support of South African search and rescue operations at sea. J. Operat. Oceanography 1–9.
Hsu, P.C., Zheng, Q., Lu, C.Y., Cheng, K.H., Lee, H.J., Ho, C.R., 2018. Interaction of coastal countercurrent in I-lan bay with the Kuroshio northeast of taiwan. Continent. Shelf Res. 171, 30–41.
Hutchings, L., Beckley, L., Griffiths, M., Roberts, M., Sundby, S., Van der Lingen, C., 2002. Spawning on the edge: spawning grounds and nursery areas around the southern African coastline. Mar. Freshw. Res. 53, 307–318.
Hutchinson, K., Beal, L.M., Penven, P., Ansorge, I., Hermes, J., 2018. Seasonal phasing of Agulhas current transport tied to a baroclinic adjustment of near-field winds. J. Geophys. Res.: Oceans 123, 7067–7083.
Hyun, K.H., He, R., 2010. Coastal upwelling in the South Atlantic Bight: a revisit of the 2003 cold event using long term observations and model hindcast solutions. J. Mar. Syst. 83, 1–13.
Ingham, M.C., 1970. Coastal upwelling in the northwestern Gulf of Guinea. Bull. Mar. Sci. 20, 1–34.
Krug, M., Penven, P., 2011. New perspectives on Natal Pulses from satellite observations. J. Geophys. Res.: Oceans 116.
Krug, M., Tournadre, J., 2012. Satellite observations of an annual cycle in the Agulhas Current. Geophys. Res. Lett. 39.
Krug, M., Swart, S., Gula, J., 2017. Submesoscale cyclones in the Agulhas current. Geophys. Res. Lett. 44, 346–354.
Lamont, T., Louw, G., Russo, C., van den Berg, M., 2021. Observations of northeastward flow on a narrow shelf dominated by the Agulhas Current. Estuarine. Coast. Shelf Sci. 251, 107197.
Lange, M., Sebille, E.v., 2017. Parcels v0. 9: prototyping a Lagrangian ocean analysis framework for the petascale age. Geosci. Model Dev. (GMD) 10, 4175–4186.
Le Gouvello, D.Z., Hart-Davis, M.G., Backeberg, B.C., Nel, R., 2020. Effects of swimming behaviour and oceanography on sea turtle hatchling dispersal at the intersection of two ocean current systems. Ecol. Model. 431, 109130.
Lee, T.N., Yoder, J.A., Atkinson, L.P., 1991. Gulf Stream frontal eddy influence on productivity of the southeast US continental shelf. J. Geophys. Res.: Oceans 96, 22191–22205.
Leis, J.M., 2006. Are larvae of demersal fishes plankton or nekton? Adv. Mar. Biol. 51, 57–141.
Lemasson, L., Rebert, J.P., 1968. Observations de courants sur le plateau continental ivoirien Mise en évidence d'un sous-courant. Centre de Recherches Océanographiques.
Lima, I.D., Garcia, C.A., Möller, O.O., 1996. Ocean surface processes on the southern Brazilian shelf: characterization and seasonal variability. Continent. Shelf Res. 16, 1307–1317.
Luiz, O.J., Allen, A.P., Robertson, D.R., Floeter, S.R., Kulbicki, M., Vigliola, L., Becheler, R., Madin, J.S., 2013. Adult and larval traits as determinants of geographic range size among tropical reef fishes. Proc. Natl. Acad. Sci. USA 110, 16498–16502.
Lutjeharms, J., Roberts, H., 1988. The Natal pulse: an extreme transient on the Agulhas Current. J. Geophys. Res.: Oceans 93, 631–645.
Meyer, A., Lutjeharms, J., De Villiers, S., 2002. The nutrient characteristics of the Natal Bight, South Africa. J. Mar. Syst. 35, 11–37.
Nagano, A., Yamashita, Y., Hasegawa, T., Ariyoshi, K., Matsumoto, H., Shinohara, M., 2019. Characteristics of an atypical large-meander path of the Kuroshio current south of Japan formed in September 2017. Mar. Geophys. Res. 40, 525–539.
Nelson, G., Hutchings, L., 1983. The Benguela upwelling area. Prog. Oceanogr. 12, 333–356.
North, E.W., Schlag, Z., Hood, R.R., Li, M., Zhong, L., Gross, T., Kennedy, V.S., 2008. Vertical swimming behavior influences the dispersal of simulated oyster larvae in a coupled particle-tracking and hydrodynamic model of Chesapeake Bay. Mar. Ecol. Prog. Ser. 359, 99–115.
Oliff, W., 1969. The Disposal of Effluents into the Sea off the Natal Coast. Pietermaritzburg, the town.
Pearce, A.F., Af, P., 1977. The Shelf Circulation off the East Coast of South Africa.
Pfaff, M.C., Hart-Davis, M., Smith, M.E., Veitch, J., 2022. A new model-based coastal retention index (CORE) identifies bays as hotspots of retention, biological production and cumulative anthropogenic pressures. Estuar. Coast Shelf Sci., 107909
Pitts, P.A., Smith, N.P., 1997. An investigation of summer upwelling across central Florida's Atlantic coast: the case for wind stress forcing. JCR (J. Coast. Res.) 105–110.
Roberts, M., Nieuwenhuys, C., 2016. Observations and mechanisms of upwelling in the northern KwaZulu-Natal Bight, South Africa. Afr. J. Mar. Sci. 38, S43–S63.
Roberts, M., Van der Lingen, C., Whittle, C., Van den Berg, M., 2010. Shelf currents, lee-trapped and transient eddies on the inshore boundary of the Agulhas Current, South Africa: their relevance to the KwaZulu-Natal sardine run. Afr. J. Mar. Sci. 32, 423–447.
Roberts, M., Zemlak, T., Connell, A., 2011. Cyclonic eddies reveal Oegopsida squid egg balloon masses in the Agulhas Current, South Africa. Afr. J. Mar. Sci. 33, 239–246.
Roberts, M., Nieuwenhuys, C., Guastella, L., 2016. Circulation of shelf waters in the KwaZulu-natal Bight, South Africa. Afr. J. Mar. Sci. 38, S7–S21.
Roughan, M., Middleton, J.H., 2002. A comparison of observed upwelling mechanisms off the east coast of Australia. Continent. Shelf Res. 22, 2551–2572.
Roughan, M., Middleton, J.H., 2004. On the East Australian Current: variability, encroachment, and upwelling. J. Geophys. Res.: Oceans 109.
Roullet, G., Capet, X., Maze, G., 2014. Global interior eddy available potential energy diagnosed from Argo floats. Geophys. Res. Lett. 41, 1651–1656.
Sale, P.F., Cowen, R.K., Danilowicz, B.S., Jones, G.P., Kritzer, J.P., Lindeman, K.C., Planes, S., Polunin, N.V., Russ, G.R., Sadovy, Y.J., et al., 2005. Critical science gaps impede use of no-take fishery reserves. Trends Ecol. Evol. 20, 74–80.
Scharler, U., Ayers, M., de Lecea, A., Pretorius, M., Fennessy, S., Huggett, J., MacKay, C., Muir, D., 2016. Riverine influence determines nearshore heterogeneity of nutrient (c, n, p) content and stoichiometry in the KwaZulu-Natal Bight, South Africa. Afr. J. Mar. Sci. 38, S193–S203.
Schumann, E., 1981. Low frequency fluctuations off the Natal coast. J. Geophys. Res.: Oceans 86, 6499–6508.
Schumann, E., 1987. The coastal ocean off the east coast of South Africa. Trans. Roy. Soc. S. Afr. 46, 215–229.
Shchepetkin, A.F., McWilliams, J.C., 2005. The regional oceanic modeling system (roms): a split-explicit, free-surface, topography-following-coordinate oceanic model. Ocean Model. 9, 347–404.
Soloviev, A.V., Hirons, A., Maingot, C., Dean, C.W., Dodge, R.E., Yankovsky, A.E., Wood, J., Weisberg, R.H., Luther, M.E., McCreary, J.P., 2017. Southward flow on the western flank of the Florida Current. Deep Sea Res. Oceanogr. Res. Pap. 125, 94–105.
Tedesco, P., Gula, J., Ménesguen, C., Penven, P., Krug, M., 2019. Generation of submesoscale frontal eddies in the Agulhas Current. J. Geophys. Res.: Oceans 124, 7606–7625.
Tedesco, P., Gula, J., Penven, P., Ménesguen, C., 2022. Mesoscale eddy kinetic energy budgets and transfers between vertical modes in the Agulhas current. J. Phys. Oceanogr. 52, 677–704.